Electronic Supplementary Information

Peroxidase-Like Activity of MoS_2 Nanoflakes with Different Modifications and Their Application for H_2O_2 and Glucose Detection

Jie Yu [a,b], Dongqing Ma[b], Linqiang Mei[b], Qin Gao[b], Wenyan Yin[b,*], Xiao Zhang[b], Liang Yan[b], Zhanjun Gu[b,*], Xiaoyan Ma[a,*], and Yuliang Zhao[b]

[a]Key Laboratory of Polymer Science and Technology, School of Science, Northwestern Polytechnical University, Xi'an, Shaanxi, 710129, P. R. China

[b]Key Laboratory for Biomedical Effects of Nanomaterials and Nanosafety, Institute of High Energy Physics, Chinese Academy of Sciences, Beijing 100049, P. R. China

*Corresponding Authors E-mail: yinwy@ihep.ac.cn, zjgu@ihep.ac.cn, m_xiao_yana@nwpu.edu.cn,

The descriptions about interactions between the MoS_2 and functionalization molecules:

There are three types of interaction between MoS_2 and functionalization molecules, including electrostatic interaction (PEI-MoS_2), hydrophilic/hydrophobic interaction (PVP-MoS_2, or PAA-MoS_2), and covalent interaction (Cys-MoS_2). Briefly, (1) for MoS_2-Cys, the S vacancy could exist in 2H and 1T phases of MoS_2, which are all layered structure except for the different atomic arrangement of S in their crystal phase.[1] Therefore, the S vacancy provided an active site to form covalent bond between Cys and MoS_2 via thiol group;[2] (2) For MoS_2-PEI, due to the negatively charged MoS_2 with 1T and 2H phase, the PEI molecule with positive charge can adsorb onto the surface of MoS_2 NFs via electrostatic interaction; (3) For PVP- or PAA-MoS_2, the hydrophobic alkyl chains in PVP and PAA molecule provided hydrophilic/hydrophobic interaction between MoS_2 and PAA/PVP, thus the mixed phase of MoS_2 were involved and hydrophobic interaction may play a key role in PAA- and PVP- MoS_2 NFs.

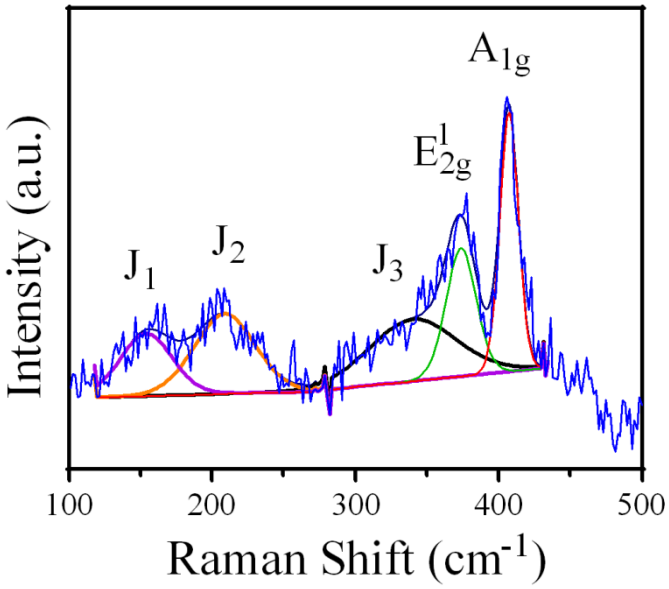

Fig. S1. Raman spectrum of MoS_2 NFs. The peaks of J_1, J_2, and J_3 were attributed to the 1T phase of MoS_2.

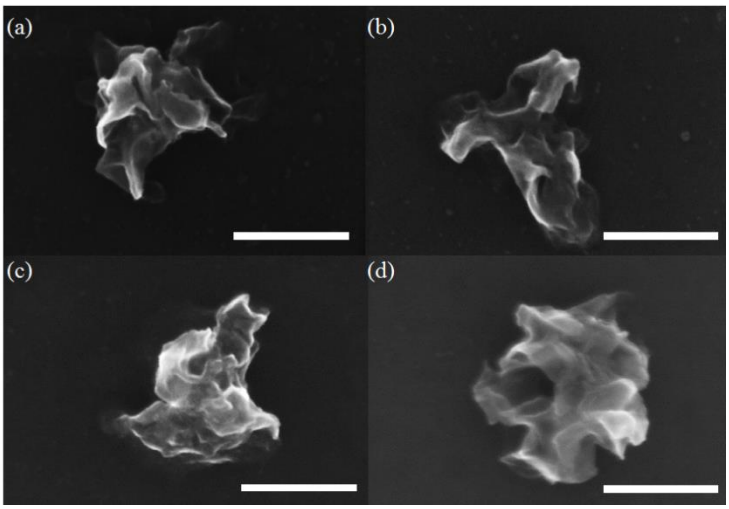

Fig. S2. FE-SEM images of (a) PVP-MoS_2, (b) PEI-MoS_2, (c) PAA-MoS_2, and (d) Cys-MoS_2. Scale bar: 200 nm.

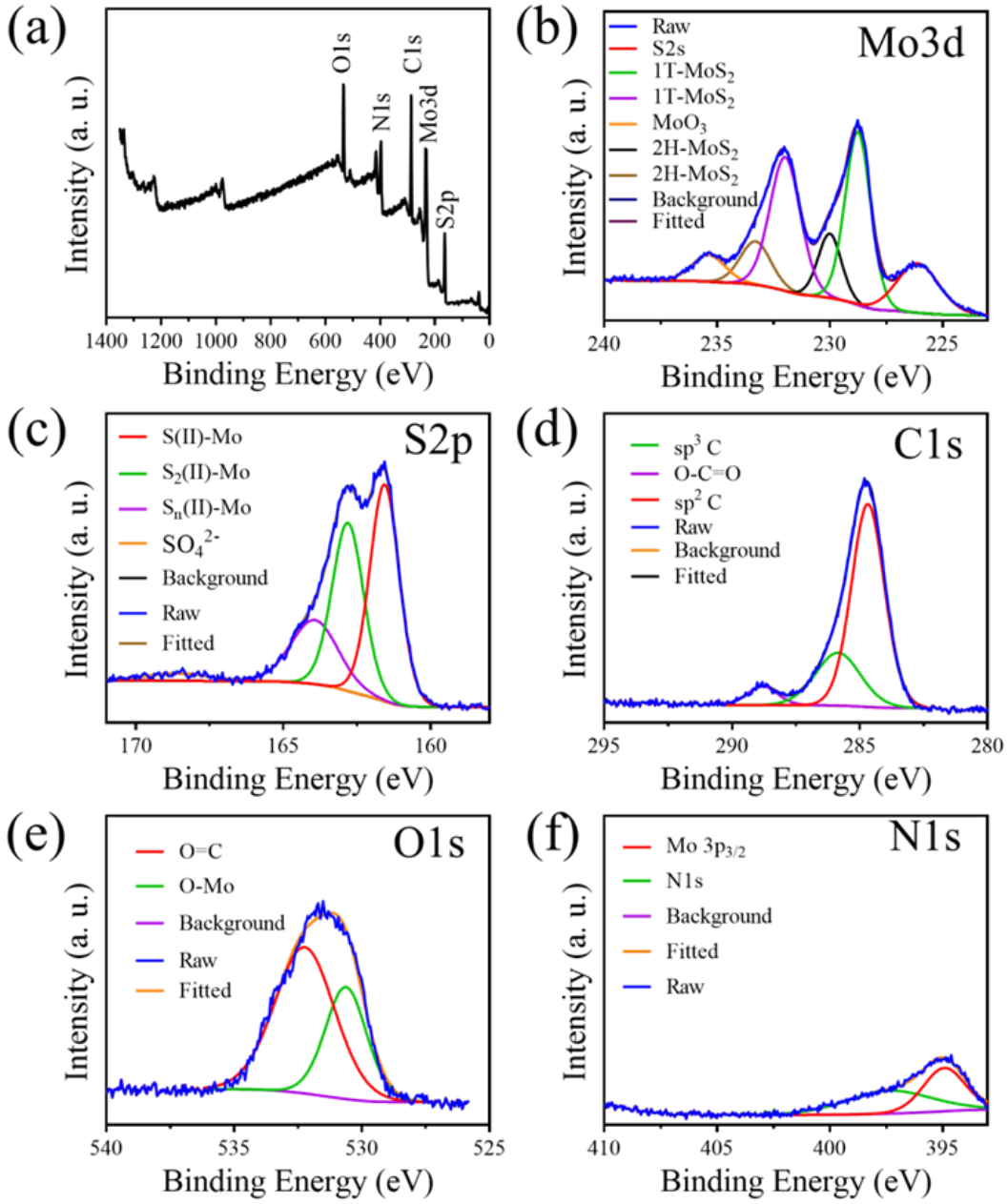

Fig. S3. XPS spectra of MoS_2 NFs. (a) Survey plot, (b-f) high-resolution XPS spectra: (b) Mo3d, (c) S2p, (d) C1s, (e) O1s, and (f) N1s.

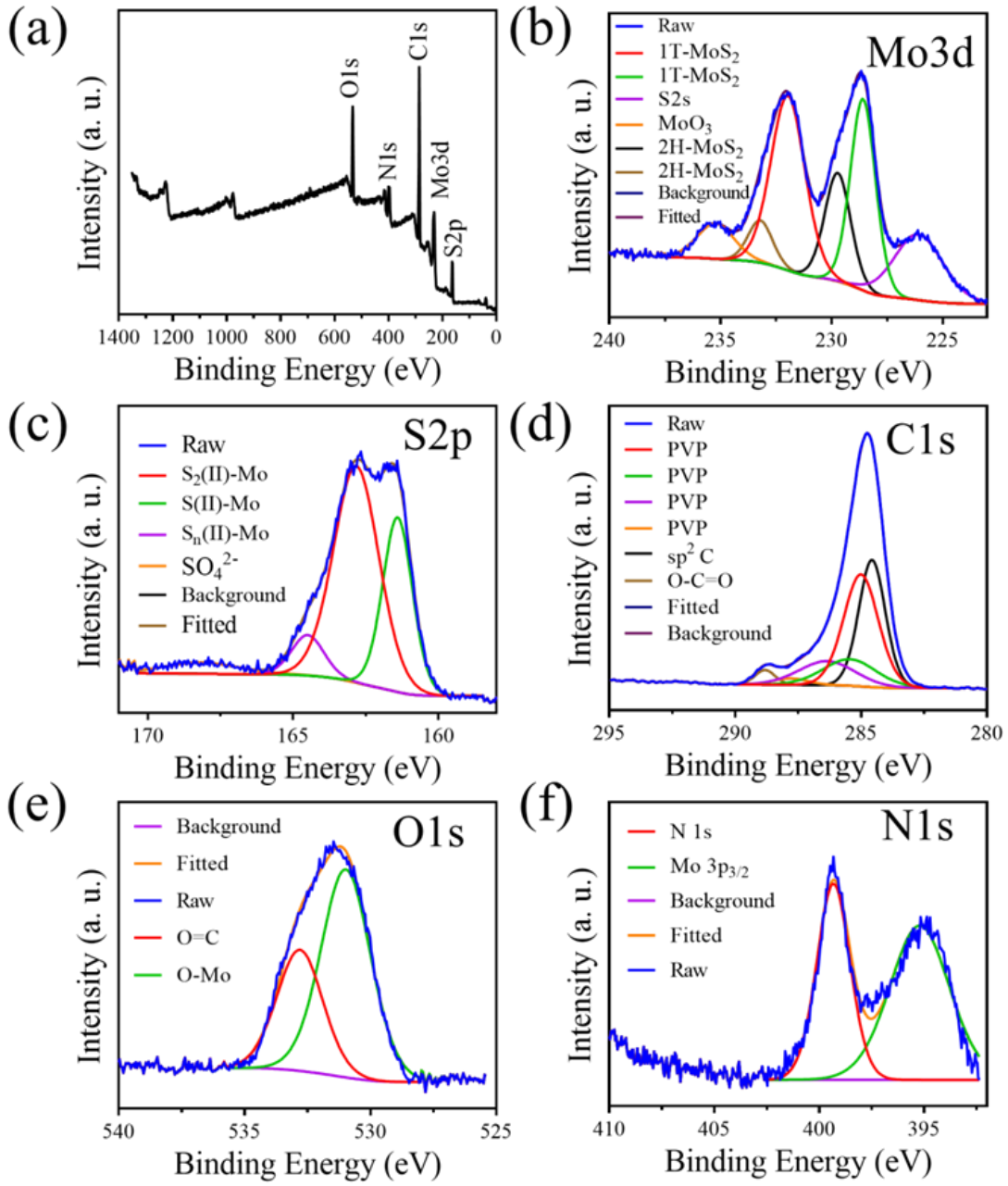

Fig. S4. XPS spectra of PVP-MoS_2 NFs. (a) Survey plot, (b-f) high-resolution XPS spectra: (b) Mo3d, (c) S2p, (d) C1s, (e) O1s, and (f) N1s.

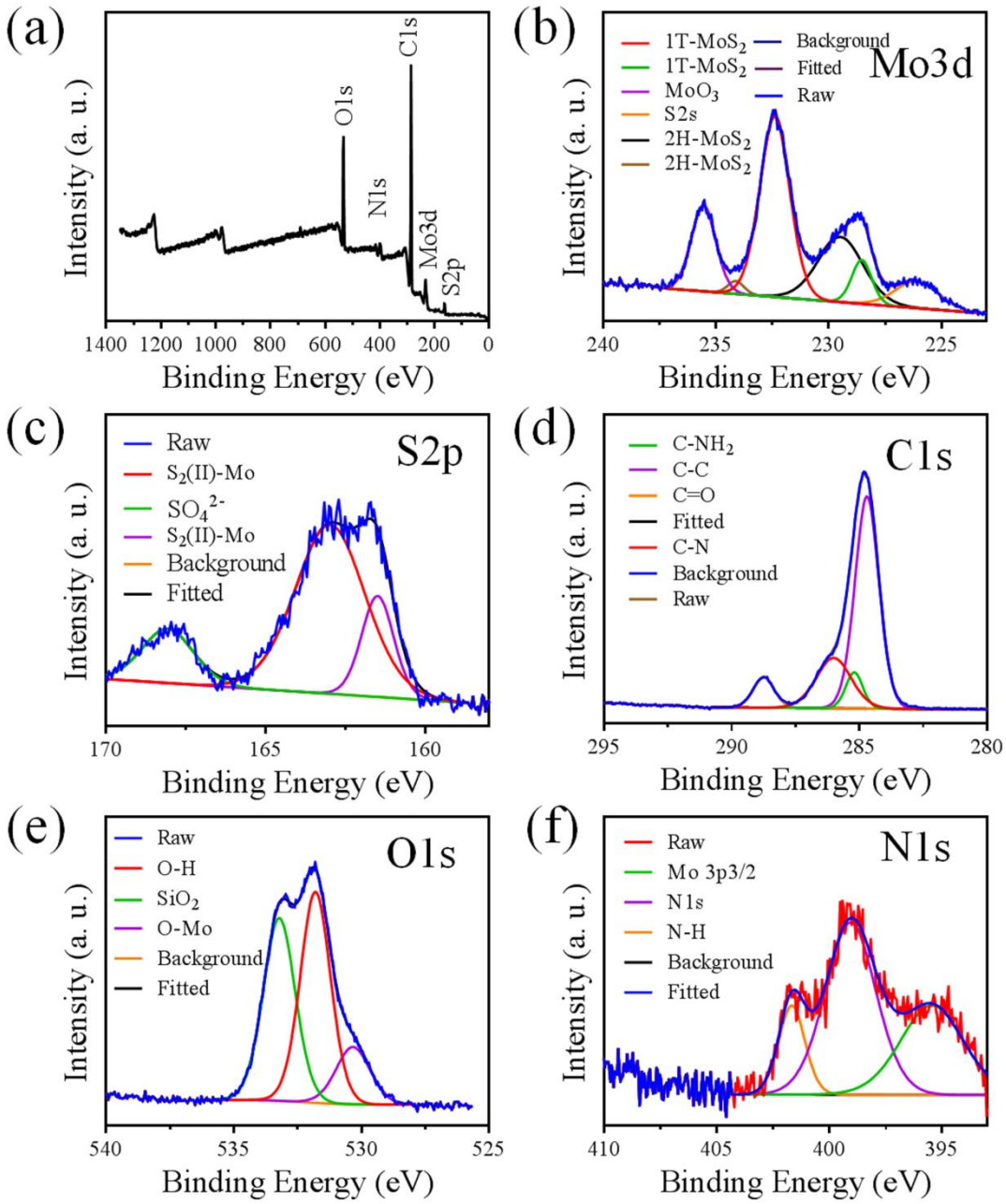

Fig. S5. XPS spectra of PEI-MoS_2 NFs. (a) Survey plot, (b-f) high-resolution XPS spectra: (b) Mo3d, (c) S2p, (d) C1s, (e) O1s, and (f) N1s.

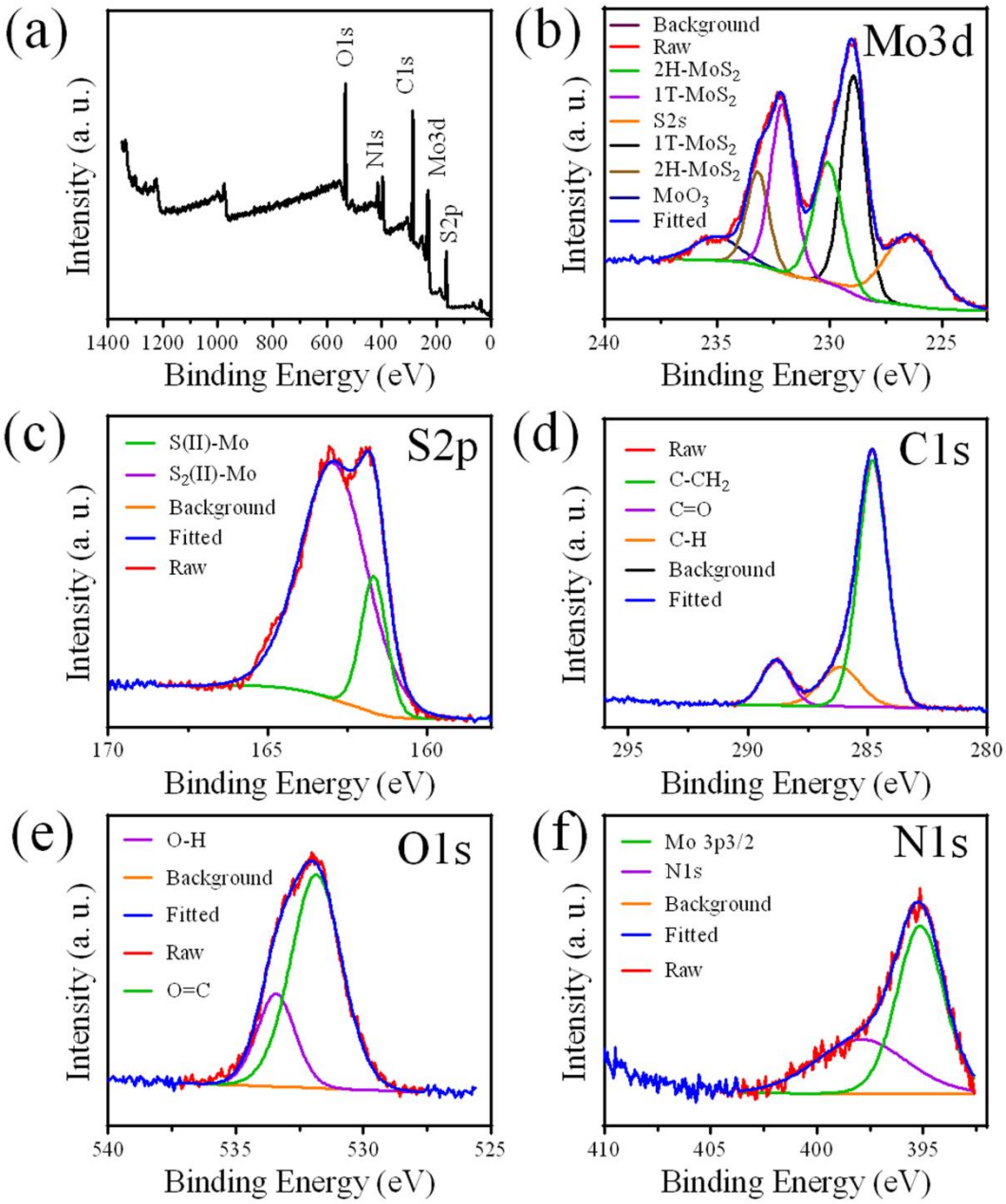

Fig. S6. XPS spectra of PAA-MoS_2 NFs. (a) Survey plot, (b-f) high-resolution XPS spectra: (b) Mo3d, (c) S2p, (d) C1s, (e) O1s, and (f) N1s.

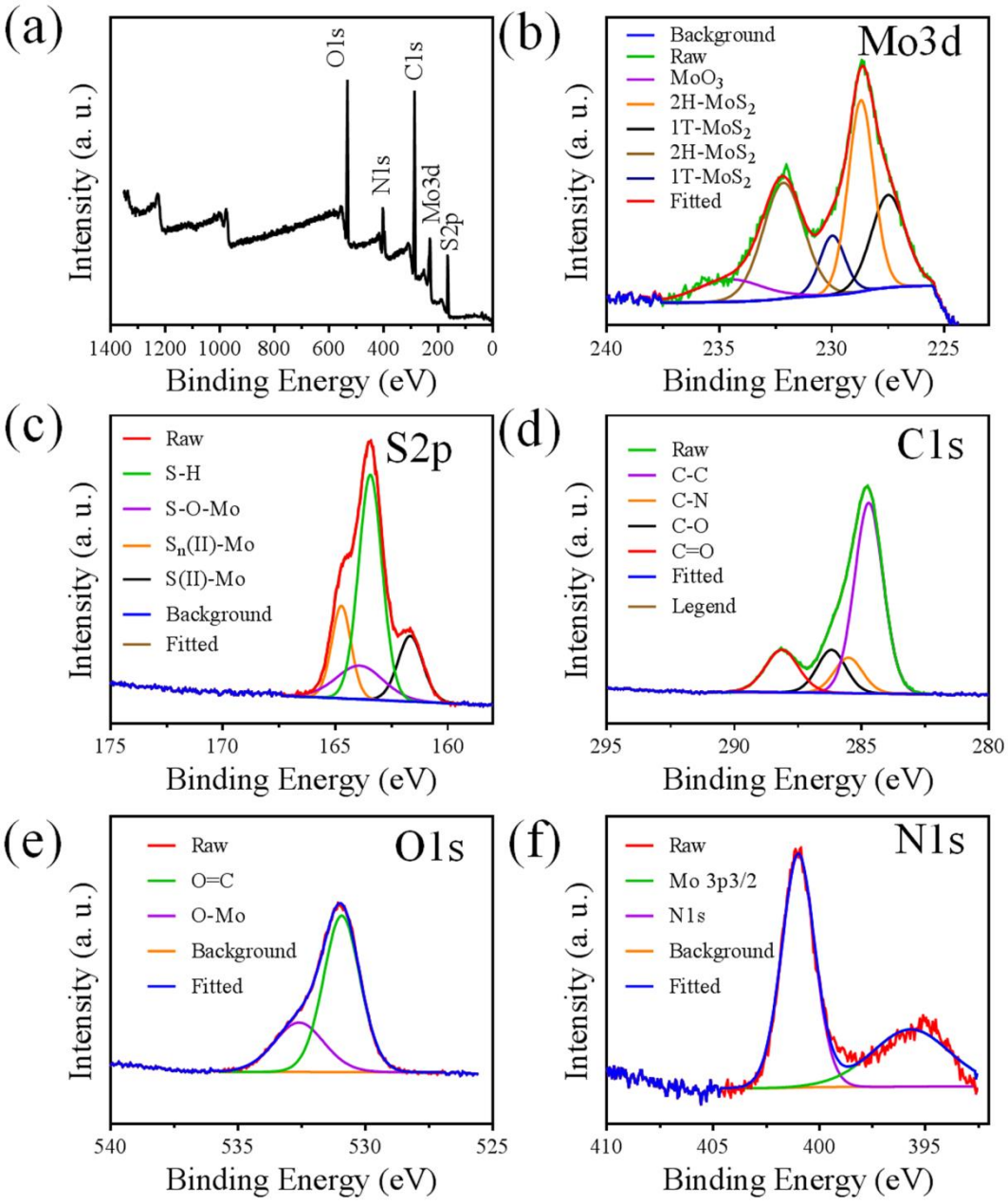

Fig. S7. XPS spectra of Cys-MoS_2 NFs. (a) Survey plot, (b-f) high-resolution XPS spectra: (b) Mo3d, (c) S2p, (d) C1s, (e) O1s, and (f) N1s.

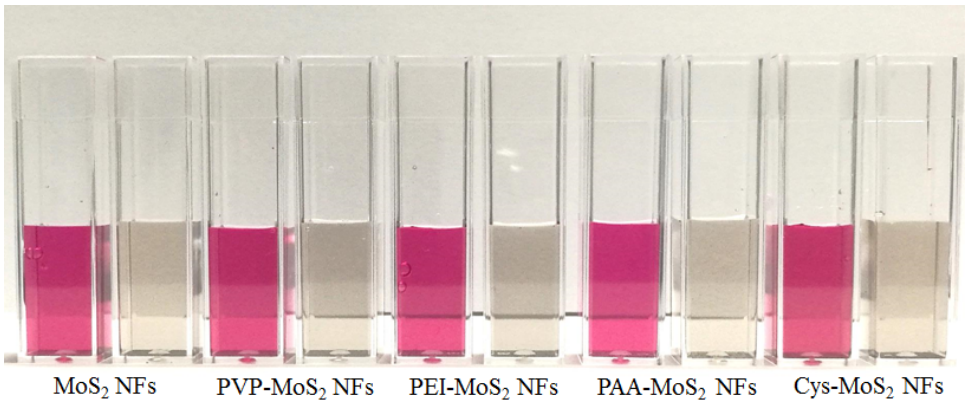

Fig. S8. Stability tests of MoS_2 NFs and modified MoS_2 NFs in DMEM (left) and water (right) solutions. The concentration of each MoS_2 NFs solution was 100 μg mL^{-1}.

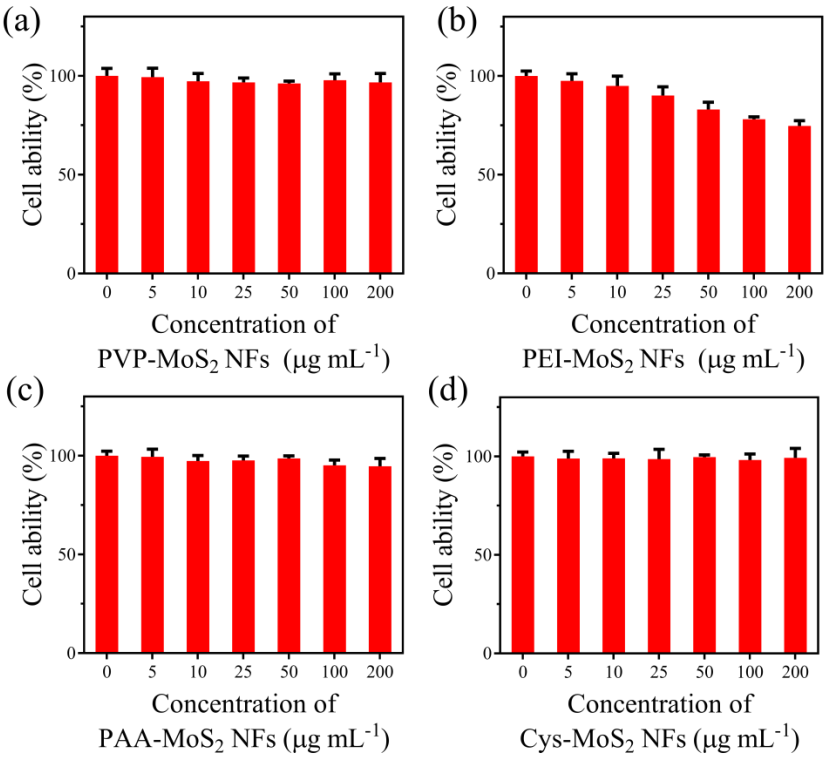

Fig. S9. Cell viabilities of (a) PVP-MoS_2 NFs, (b) PEI-MoS_2, (c) PAA-MoS_2 NFs, and (d) Cys-MoS_2 NFs after incubation with HUVEC cells for 24 h.

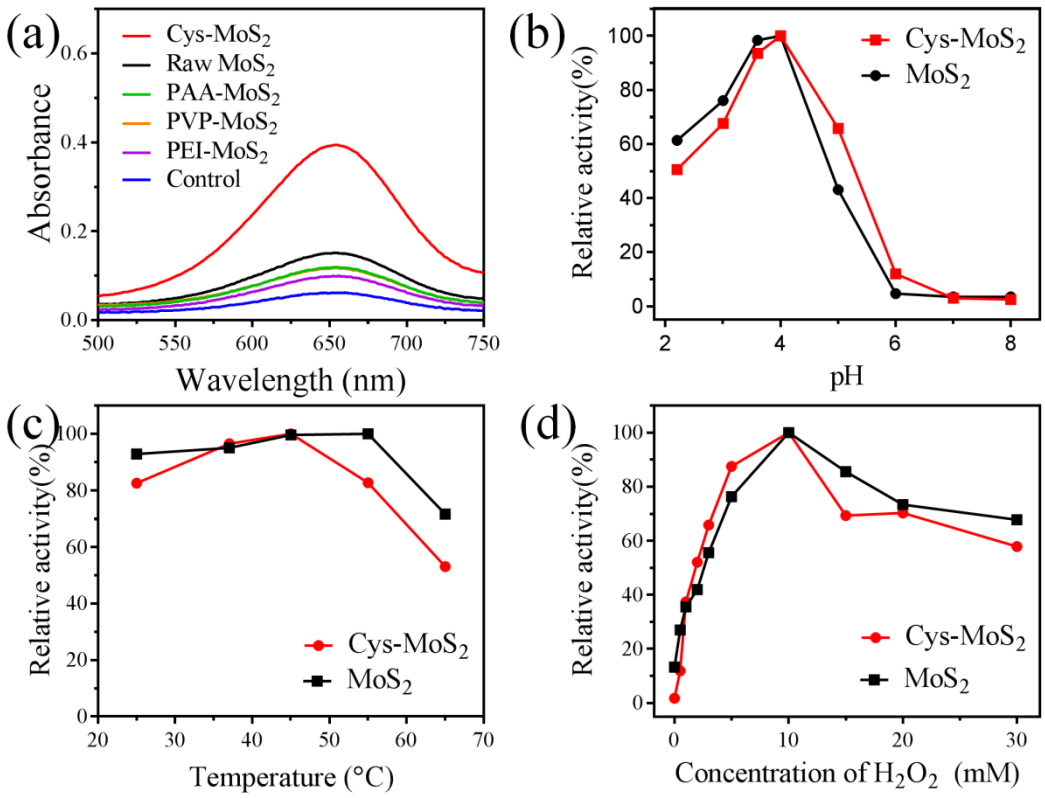

Fig. S10. Peroxidase-like catalytic activity of MoS_2 NFs toward TMB with or without modifications. (a) UV-Vis spectra of raw MoS_2 NFs and modified MoS_2 NF. (b) pH- and (c) temperature-dependent activities of MoS_2 NFs and Cys-MoS_2 NFs. (d) H_2O_2 concentration-dependent peroxidase activity of MoS_2 NFs and Cys-MoS_2 NFs. The concentrations of NFs and TMB were respectively 33 μg mL^{-1} and 1 mM for all the experiment. The concentration of H_2O_2 for absorbance, pH and temperature measurements was 10 mmol L^{-1}. The solution containing 1 mM of TMB and 10 mM of H_2O_2 was used as control.

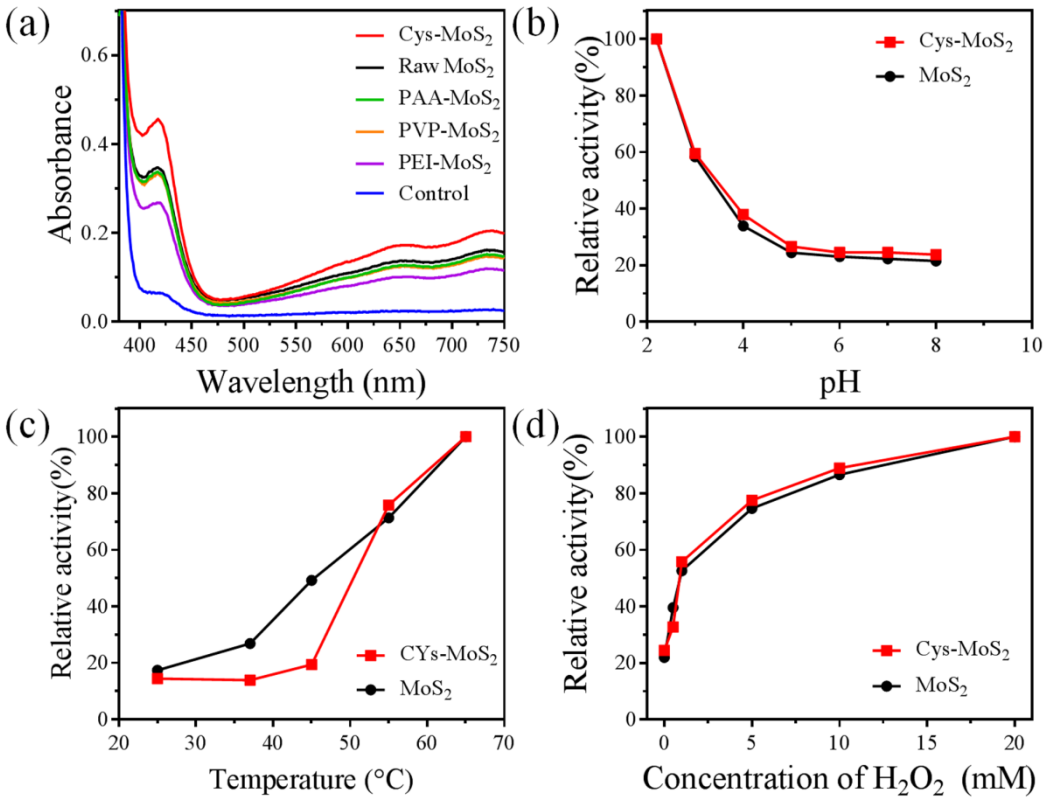

Fig. S11. Peroxidase-like catalytic activity of MoS_2 NFs toward ABTS with or without modifications. (a) UV-Vis spectra of raw MoS_2 NFs and modified MoS_2 NFs. (b) pH- and (c) temperature-dependent activities of MoS_2 NFs and Cys-MoS_2 NFs. (d) H_2O_2 concentration-dependent peroxidase-like catalytic activity of MoS_2 NFs and Cys-MoS_2 NFs. The concentrations of NFs and ABTS were respectively 33 μg mL^{-1} and 1 mM for all the experiment. The concentration of H_2O_2 for absorbance, pH and temperature measurements was 10 mM. The solution containing 1 mM of ABTS and 10 mM of H_2O_2 was used as control.

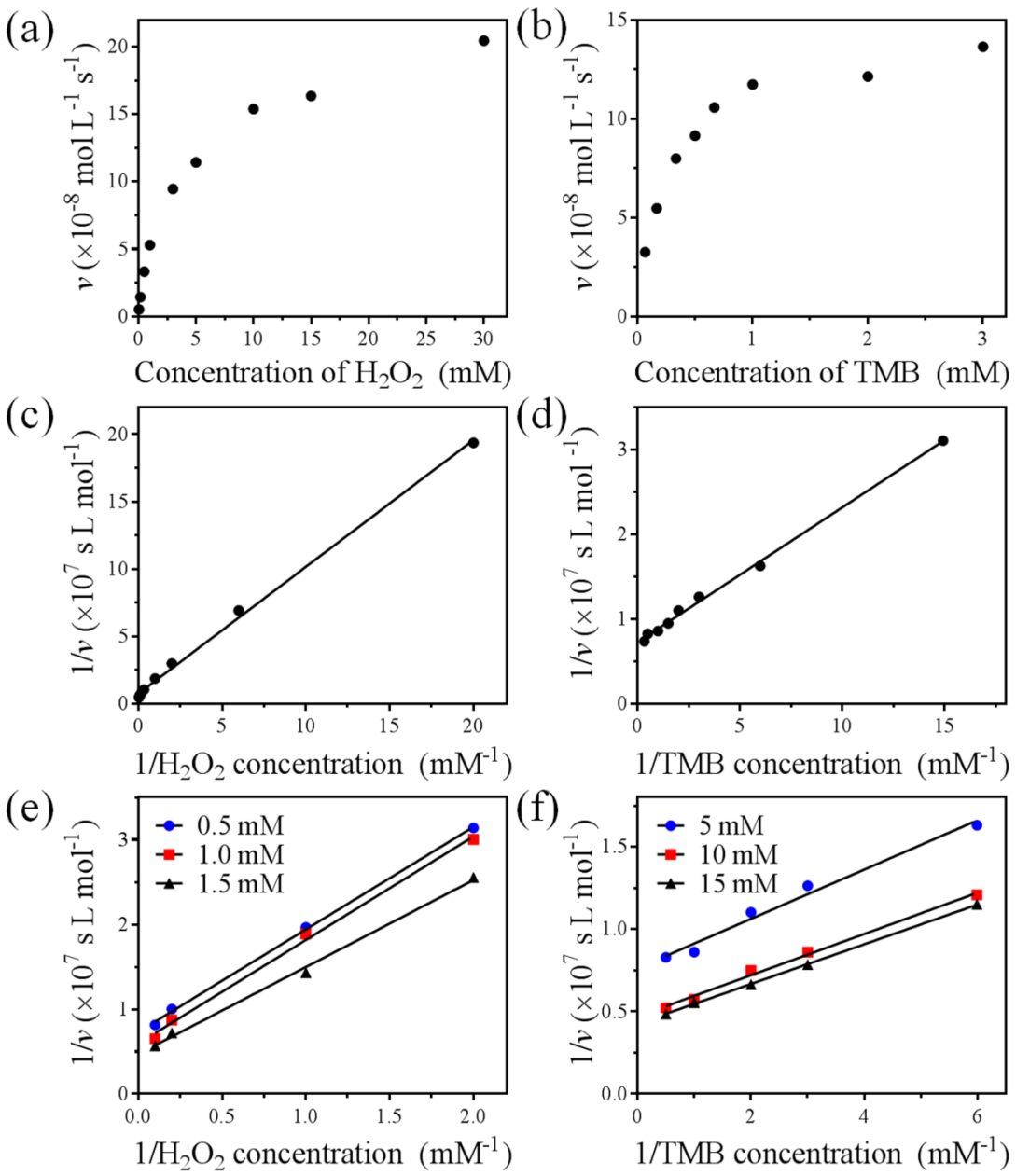

Fig. S12. Steady-state kinetic assay and catalytic mechanism of raw MoS_2 NFs. The velocity was determined by measuring the absorbance of oxidized TMB under different (a) H_2O_2 and (b) TMB concentrations. (c-d) Corresponding double-reciprocal plots of MoS_2 NFs at a fixed concentration of one substrate *versus* varying the concentration of another (c) H_2O_2 or (d) TMB. (e-f) Lineweaver-Burk plots of raw MoS_2 NFs at each concentration of one substrate versus varying concentration of another substrate.

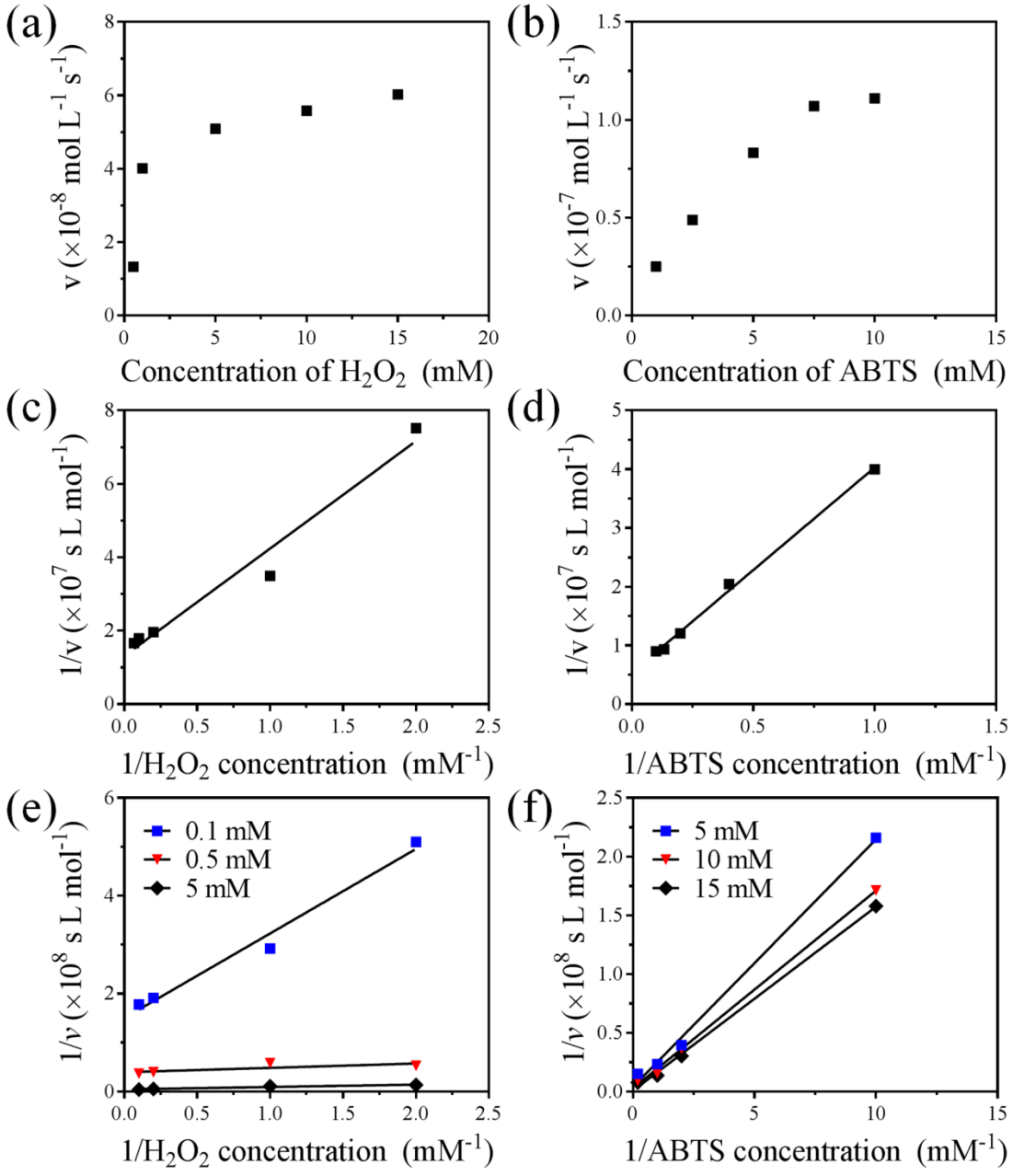

Fig. S13. Steady-state kinetic assay and catalytic mechanism of raw MoS_2 NFs. The velocity was determined by measuring the absorbance of oxidized ABTS under different (a) H_2O_2 and (b) ABTS concentrations. (c-d) Corresponding double-reciprocal plots of MoS_2 NFs at a fixed concentration of one substrate *versus* varying the concentration of (c) H_2O_2 or (d) ABTS. (e-f) Lineweaver-Burk plots of MoS_2 NFs at each concentration of one substrate versus varying concentration of another substrate.

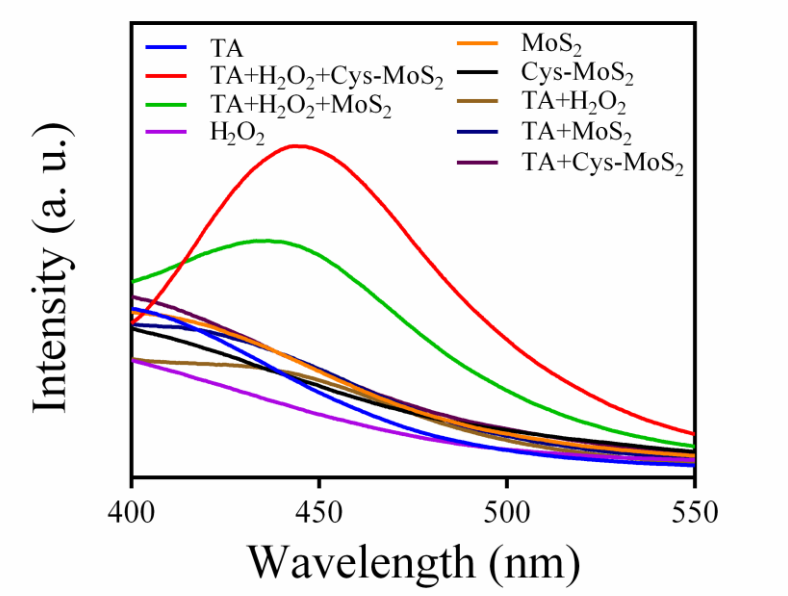

Fig. S14. TA as fluorescent probe to test the formation of ·OH at pH = 4.0. Reaction conditions: 1.0 μg mL^{-1} of Cys-MoS_2 and MoS_2, 100 μM of H_2O_2, 0.5 mM of TA, and 0.1 M acetate buffer (pH = 4.0) at 25 ºC for 12 h.

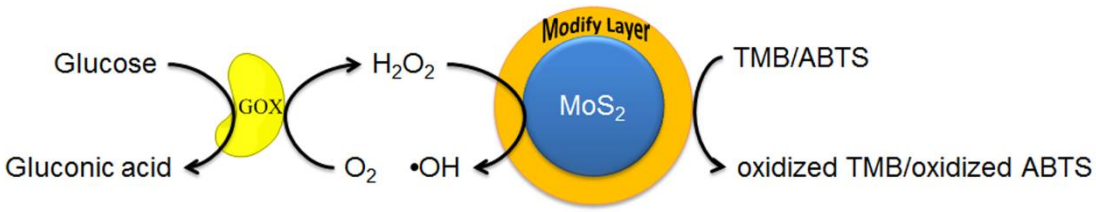

Scheme S1. Illustration of MoS_2 NFs and Cys-MoS_2 NFs used for H_2O_2 and glucose detection.

Table S1. Comparisons of various methods for glucose detection.

Materials	Method	Linear Range (mmol L^{-1})	Ref.
Hollow Pt/MWCNTs	electrochemistry	0.0012–8.4	3
PVP-Ag nanowires	electrochemistry	2–20	4
Cu_2O nanocubes/graphene	electrochemistry	0.3–3.3	5
Au nanoclusters	fluorimetry	0.01- 0.5	6
B-doped carbon quantum dot	fluorimetry	0.008-0.08	7
QDs-ConA-β-CDs-AuNP	fluorimetry	0.0001-0.05	8
Fe–Phen–CFs	fluorimetry	0.0005-0.2	9
Graphene oxide	colorimetry	0.001-0.02	10
Carbon nanodots	colorimetry	0.001-0.5	11
$ZnFe_2O_4$ nanoparticles	colorimetry	0.0012-0.019	12
SDS-MoS_2	colorimetry	0.002-0.1	13
PVP-MoS_2 nanoparticles	colorimetry	1-10	14
CoOOH nanoflakes	colorimetry	0.0053–0.5	15
Porphyrin-CeO_2	colorimetry	0.019-0.15	16
MoS_2/graphene oxide	colorimetry	0.001-0.05	17
MoS_2 NFs	colorimetry	0.1-1	This work
Cys-MoS_2 NFs	colorimetry	0.05-1	This work

References

1. D. Voiry, A. Mohite and M. Chhowalla, *Chem. Soc. Rev.*, 2015, **44**, 2702-2712.
2. S. S. Chou, M. De, J. Kim, S. Byun, C. Dykstra, J. Yu, J. Huang and V. P. Dravid, *J. Am. Chem. Soc.*, 2013, **135**, 4584-4587.
3. Y. Wang, R. Yuan, Y. Chaia, W. Li, Y. Zhuo, Y. Yuan and J. Li, *J. Mol. Catal. B: Enzym.*, 2011, **71**, 146-151.
4. X. Yang, J. Bai, Y. Wang, X. Jiang and X. He, *Analyst*, 2012, **137**, 4362-4367.
5. M. Liu, R. Liu and W. Chen, *Biosens. Bioelectron.*, 2013, **45**, 206-212.
6. L. Jin, L. Shang, S. Guo, Y. Fang, D. Wen, L. Wang, J. Yin and S. Dong, *Biosens. Bioelectron.*, 2011, **26**, 1965-1969.
7. X. Shan, L. Chai, J. Ma, Z. Qian, J. Chen and H. Feng, *Analyst*, 2014, **139**, 2322-2325.
8. B. Tang, L. Cao, K. Xu, L. Zhuo, J. Ge, Q. Li and L. Yu, *Chem. - Eur. J.*, 2008, **14**, 3637-3644.
9. X. Zhu, J. Xiang, J. Li, C. Feng, P. Liu and B. Xiang, *J. Colloid Interface Sci.*, 2018, **511**, 209-214.
10. Y. Song, K. Qu, C. Zhao, J. Ren and X. Qu, *Adv. Mater.*, 2010, **22**, 2206-2210.
11. W. Shi, Q. Wang, Y. Long, Z. Cheng, S. Chen, H. Zheng and Y. Huang, *Chem. Commun.*, 2011, **47**, 6695-6697.
12. L. Su, J. Feng, X. Zhou, C. Ren, H. Li and X. Chen, *Anal. Chem.*, 2012, **84**, 5753-5758.

13. K. Zhao, W. Gu, S. Zheng, C. Zhang and Y. Xian, *Talanta*, 2015, **141**, 47-52.
14. J. Yu, X. Y. Ma, W. Y. Yin and Z. J. Gu, *RSC Adv.*, 2016, **6**, 81174-81183.
15. Y. Wang, X. Shen and F. Chen, *Journal of Molecular Catalysis A: Chemical*, 2014, **381**, 38-45.
16. J. R. Lince, A. M. Pluntze, S. A. Jackson, G. Radhakrishnan and P. M. Adams, *Tribology Letters*, 2014, **53**, 543-554.
17. J. Cao, X. Zhang, Y. Zhang, J. Zhou, Y. Chen and X. Liu, *PLOS ONE*, 2016, DOI: 10.1371/journal.pone.0161374.